Journal of Inorganic and General Chemistry
ZAAC
Zeitschrift für anorganische und allgemeine Chemie
www.zaac.wiley-vch.de
RESEARCH ARTICLE
Check for updates
DOI: 10.1002/zaac.202500088

Terbium Carbazolate: Synthesis with Terbium Nanoparticles, Structure, and Luminescence

Andreas Reiß, Jule J. Baur, Radian Popescu, Yolita M. Eggeler, and Claus Feldmann*

Dedicated to Professor Mathias Wickleder on the occasion of his 60th birthday

Zerovalent Terbium metal nanoparticles are prepared in the liquid phase by reduction of $TbCl_3$ with lithium naphthalenide ([LiNaph]) in THF. The as-prepared Tb(0) nanoparticles are monocrystalline with small and uniform size of 2.8 ± 0.4 nm. Although the deep black Tb(0) nanoparticle suspension is colloidally and chemically stable in THF under inert conditions, it shows high reactivity when in contact with O_2, H_2O, or other oxidizing agents. The high reactivity can be used to react Tb(0) nanoparticles with carbazole (cbzH) as a sterically demanding N–H-acidic amine. As a result, Terbium carbazolate with a composition $[Tb(cbz)_3(THF)_2](cbzH)(C_7H_8)$ (**1**) is obtained upon oxidation of Terbium and formation of H_2. Herein, Tb^{3+} is coordinated by three deprotonated, negatively charged $(cbz)^-$ ligands and two molecules of THF. Already in daylight, **1** shows Tb^{3+}-driven emission of green light with cbz serving as an antenna for excitation. The Tb(0) nanoparticles and the Terbium carbazolate **1** are characterized by transmission electron microscopy, electron diffraction, Fourier transform infrared spectroscopy, crystal-structure analysis, and photoluminescence spectroscopy.

1. Introduction

Carbazole (CbzH) and its derivatives are widely applied ligands in coordination chemistry and metalorganic chemistry.[1] In detail, their relevance is substantiated by compounds with interesting bonding and coordination scenarios, luminescent and electroluminescent properties, catalysis, and supramolecular structures.[1,2] Most often, carbazole and its derivatives were used as pincer ligands to coordinate single metal atoms,[1a,3] which can lead to unique bonding situations[4] as well as single-atom catalysts.[5] Since carbazoles can serve as efficient antenna ligands, their metal complexes, specifically with metals such as Iridium or Rhodium, are intensely discussed for electroluminescence applications.[6] Finally, supramolecular structures with carbazole derivatives as linker molecules are studied with regard to gas sorption and emissive sensors.[7]

In comparison to a manifold of coordination compounds with carbazole-type ligands, the number of coordination compounds with the lanthanides is low. Here, research activities predominantly address metal organic frameworks as well as their use as emissive sensors[8] with gas sorption and gas separation properties.[9] In these compounds, the carbazole scaffold is usually functionalized with additional linker groups (most often carboxylate functionalities) that coordinate the lanthanide cation. In contrast, a homoleptic coordination of lanthanide cations by carbazole-type ligands and specifically via the central nitrogen atom is rare. In fact, homoleptic coordination of lanthanide cations by carbazole ligands was first presented in 2003 by Müller–Buschbaum.[10] Furthermore, mononuclear coordination compounds with negatively charged $(cbz)^-$ as a ligand were reported with $[(cbz)_2Sm(thf)_4]$ or $[(cbz)_2Yb(thf)_4]$.[11] In this regard, a direct reaction of the bulk-lanthanide metals with pure cbzH was already suggested and was performed, due to the low reactivity of the bulk metals, at elevated temperatures (200–400 °C).[10,12] Specifically for Terbium as a lanthanide cation, again, different 1D to 3D frameworks were reported and used for luminescence sensing and gas sorption.[13] Similar to the general situation of the lanthanides, Tb^{3+} is here usually coordinated by additional functional groups at the carbazole scaffold (e.g., carboxylate groups) instead of the central nitrogen atom.

The wide interest in coordination compounds and their properties motivated us to examine a redox approach for synthesis using reactive metal nanoparticles and carbazole at moderate temperature in the liquid phase. In regard to potential luminescence properties, we specifically used novel Terbium nanoparticles as a reactive starting material that was directly reacted with carbazole in toluene. This resulted in the formation of the Terbium carbazolate $[Tb(cbz)_3(THF)_2](cbzH)(C_7H_8)$ (**1**) with three negatively charged $(cbz)^-$ ligands and with intense Tb^{3+}-based emission.

2. Results and Discussion

2.1. Terbium Metal Nanoparticles

The realization of reactive metal nanoparticles in the liquid phase has generally attracted our attention over the last five years.

A. Reiß, J. J. Baur, C. Feldmann
Institute of Inorganic Chemistry, Karlsruhe Institute of Technology (KIT), Engesserstraße 15, D-76131 Karlsruhe, Germany
E-mail: claus.feldmann@kit.edu
R. Popescu, Y. M. Eggeler
Laboratory for Electron Microscopy, Karlsruhe Institute of Technology (KIT), Engesserstrasse 7, D-76131 Karlsruhe, Germany

Supporting information for this article is available on the WWW under https://doi.org/10.1002/zaac.202500088

After development of different synthesis strategies, such as liquid-ammonia-based microemulsions[14] and syntheses in liquid ammonia[15] or pyridine,[16] specifically the reduction of metal halides with lithium or sodium naphthalenide ([LiNaph], [NaNaph]) as powerful reducing agents in THF as the solvent turned out to be most widely applicable.[17] As a result, we could realize all group 3-to-group 6 transition metals as well as all lanthanide metals (La to Lu) as nanoparticles with a size of 1–5 nm, most of them for the first time. Among the lanthanides, we presented Tb(0) nanoparticles only recently for the first time.[18]

To obtain Tb(0) nanoparticles, an one-pot approach was used. In detail, $TbCl_3$, lithium, and naphthalene were added to THF (**Figure 1**a). After intense stirring for over 12 h at room temperature, the reaction was finished and resulted in a deep black suspension of Tb(0) nanoparticles (Figure 1b). This one-pot approach was selected due to the low solubility of $TbCl_3$ in THF. In the reaction, first of all, lithium reacts with naphthalene to lithium naphthalenide ([LiNaph]), which is indicated instantaneously after addition to THF by the occurrence of a deep green color. Thereafter, the slowly dissolving $TbCl_3$ was instantaneously reduced to elemental Terbium by the powerful reducing agent [LiNaph]. Since the dissolution of $TbCl_3$ is very slow in comparison to the reduction of Tb^{3+} to Tb(0), the one-pot approach is still suitable for preparing small-sized nanoparticles. The fact that the metal nanoparticles are highly insoluble in THF supports the nucleation of small-sized nanoparticles even further, as a high supersaturation is easily achieved. Subsequent to synthesis, the as-prepared Tb(0) nanoparticles were purified by centrifugation and repeated redispersion/centrifugation in/from THF to remove remaining starting materials, naphthalene, and LiCl. Thereafter, the Tb(0) nanoparticles can be dried in vacuum at room temperature to obtain powder samples, or they can be redispersed in THF or toluene to obtain colloidally stable suspensions.

Size and size distribution of the Tb(0) nanoparticles were investigated by transmission electron microscopy (TEM). Accordingly, overview TEM images display spherical nanoparticles with a size of 2–4 nm (**Figure 2**a). A statistical evaluation of 200 nanoparticles on different TEM images resulted in a mean particle diameter of 2.8 ± 0.4 nm (Figure 2b). High-resolution (HR)TEM images show lattice fringes extending through the whole particle and, thus, indicate the as-prepared Tb(0) nanoparticles to be monocrystalline (**Figure 3**a). The observed lattice fringes with an average distance of 3.1 ± 0.1 Å are in agreement with the lattice-plane distance of face-centered cubic bulk Terbium ($d_{-111} = 3.00$ Å).[19]

Crystallinity and structure were also confirmed by the 2D Fourier transformation (FT) analysis of a single, monocrystalline Tb(0) nanoparticle on HRTEM images (Figure 3b; SI: Figure S1, Supporting Information), which again coincides with the calculated

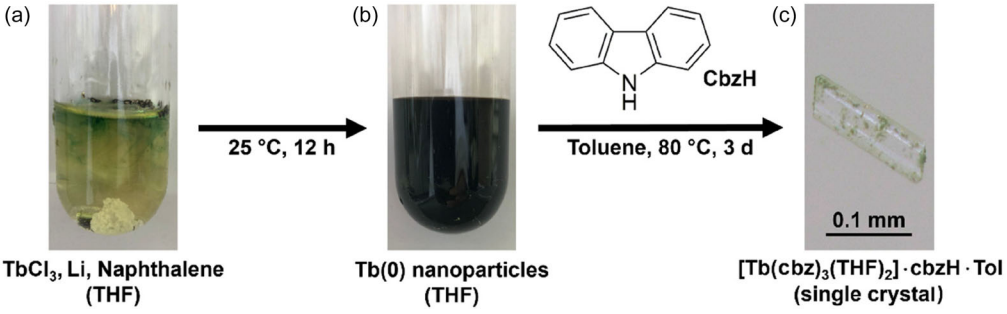

Figure 1. Scheme illustrating the synthesis of Tb(0) nanoparticles and their reaction with carbazole (cbzH): a) starting materials $TbCl_3$, lithium, and naphthalene in THF; b) suspension of Tb(0) nanoparticles in THF after the reaction; c) single crystal of $[Tb(cbz)_3(THF)_2](cbzH)(C_7H_8)$ (**1**) after reaction of Tb(0) nanoparticles with cbzH in toluene (C_7H_8).

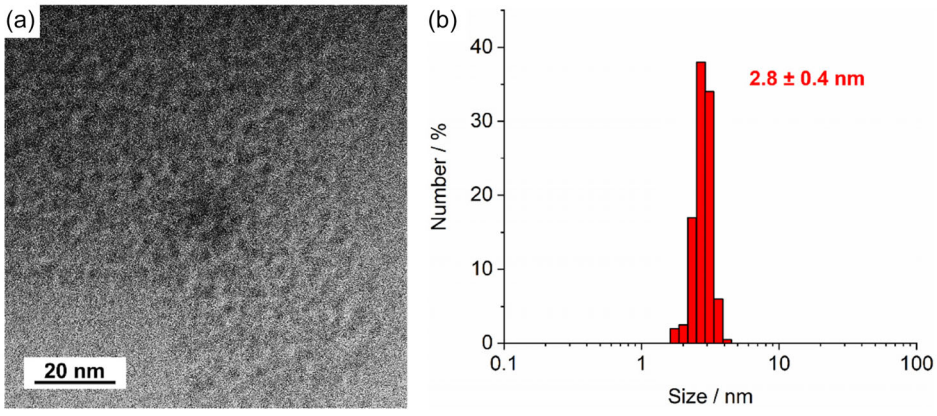

Figure 2. Size and size distribution of the as-prepared Tb(0) nanoparticles: a) TEM overview image; b) size distribution (based on statistical evaluation of 200 nanoparticles on TEM images).

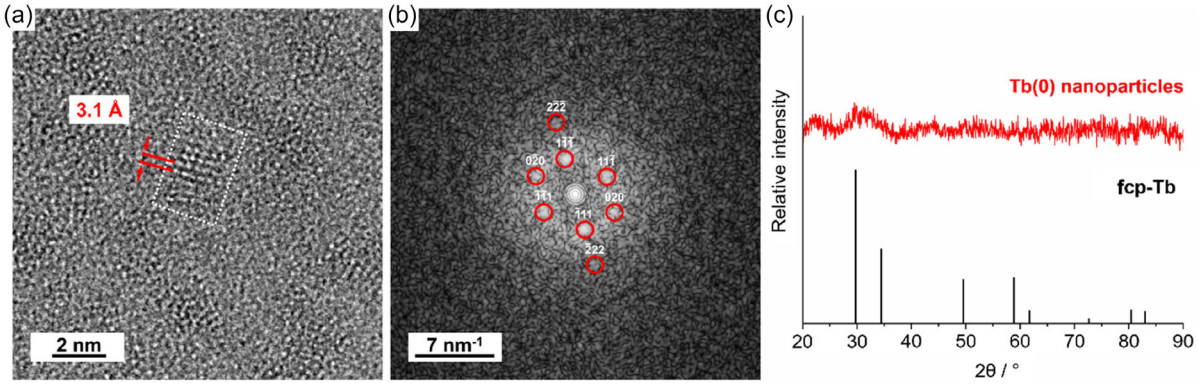

Figure 3. Crystallinity of the as-prepared Tb(0) nanoparticles: a) HRTEM image of monocrystalline Tb(0) with lattice fringes; b) FT analysis of the particle in (a) (area within dotted rectangle) with calculated diffraction patterns and Miller indices of face-centered cubic bulk Terbium in the [101]-zone axis (zero-order beam (ZB) indicated by white circle; for raw version see SI: figure S1, Supporting Information); c) XRD (with bulk Terbium as a reference: ICDD-no. 03-065−6217).

diffraction pattern of face-centered cubic bulk Terbium with a lattice parameter $a = 5.201$ Å (space group *Fm*-3*m*, in the [101]-zone axis).[19] Interestingly, bulk Terbium crystallizes with hexagonal crystal symmetry at ambient conditions and shows hexagonal closest packing (hcp) instead of the cubic closest packing (ccp) observed for the nanoparticles.[19] Notably, a ccp structure of Terbium was also observed for gas-phase evaporated Terbium thin films if the thickness is $\leq$14 nm, whereas thin films with a thickness $\geq$ 20 nm show the bulk-like hcp structure.[19] Such a difference between the crystal structure of nanomaterials and the crystal structure of the respective bulk phase at ambient conditions was frequently observed and can be ascribed to insufficient coordination of surface-allocated atoms as well as to the internal stress and strain of nanomaterials. In contrast to HRTEM, X-ray powder diffraction (XRD) of the as-prepared Tb(0) nanoparticles did not show any distinct Bragg reflection (Figure 3c). This can be attributed to the low scattering power of the small-sized Tb(0) nanoparticles in combination with the high absorption coefficient of Terbium as a heavy element. A closer view of the region around 30° of two-theta nevertheless indicates a broad, low-intensity peak at the position of the most intense Bragg reflex of the bulk, ccp-Terbium reference (Figure 3c), which also points to the presence of small crystallites. Moreover, the absence of any Bragg reflections related to LiCl indicates its complete removal after the purification of the Tb(0) nanoparticles.

The surface functionalization of the small-sized Tb(0) nanoparticles was analyzed by Fourier transform infrared (FTIR) spectroscopy and element analysis (EA). To this respect, FTIR spectra show vibrations related to THF (ν(C–H): 3000-2800 cm^{-1}, ν(C–O): 1060, 900 cm^{-1}) as well as a series of sharp vibrations at 1600-800 cm^{-1} related to naphthalene, which, as expected, is adsorbed on the surface of the Tb(0) nanoparticles (**Figure 4**a). The presence of THF and naphthalene is also confirmed by EA with C and H contents of 27.9 and 3.3 wt%, respectively. The C : H ratio of 8.5 is closer to the value

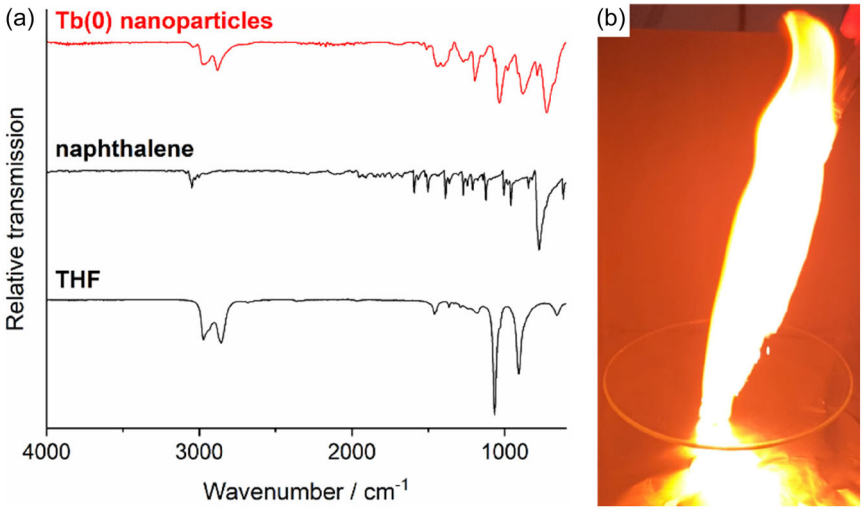

Figure 4. Surface functionalization and reactivity of the as-prepared Tb(0) nanoparticles: a) FTIR spectrum with THF and naphthalene as references; b) photo showing the reaction of Tb(0) nanoparticle-powder sample (20 mg) in air (see video SV1, Supporting Information for the reactivity in air).

of THF (6) than to naphthalene (15), indicating THF to be the predominant species adsorbed on the particle surface. This is also in agreement with previous studies.[17] Naphthalene can be removed completely if the metal nanoparticles are also redispersed/centrifuged from toluene in addition to THF.[17a,20]

Due to the small size (2.8 ± 0.4 nm), the surface functionalization with only small-sized, low-boiling molecules, and due to the absence of passivating surface layers, the Tb(0) nanoparticles can be expected to be highly reactive. Already the reaction of powder samples in air or with water evidences a high reactivity that is comparable to the heavy bulk alkali metals rubidium and cesium. Terbium powder samples, for instance, show immediate combustion when in contact with air (Figure 4b). In regard to the high reactivity, specific attention must of course be paid to all handling of the Tb(0) nanoparticles as they show instantaneous combustion in air or with other oxidizing agents (see Video SV1, Supporting Information for the reactivity in air). On the other hand, the high reactivity offers the option to perform reactions that are hardly possible with bulk Terbium.

2.2. Terbium Carbazolate

As discussed in our introduction, carbazole (cbzH) and its derivatives are interesting, sterically demanding N–H-acidic amines that are widely studied as ligands and that contribute to interesting material properties, ranging from unusual coordination scenarios via luminescence to single-atom catalysis.[1–7] This motivated us to also test the reactivity and reaction of Tb(0) nanoparticles with cbzH. In detail, the as-prepared Tb(0) nanoparticles were reacted with cbzH at 80 °C in a few drops of toluene (Figure 1c). The formation of gas bubbles indicates the reaction and formation of H_2. After three days, colorless crystals of $[Tb(cbz)_3(THF)_2](cbzH)(C_7H_8)$ (**1**) were obtained that already in daylight show luminescence with weak emission of green light. The synthesis can be rationalized with the following reaction

$$Tb(0) + 4\,cbzH + 2\,THF + C_7H_8 \rightarrow [Tb(cbz)_3(THF)_2](cbzH) \times (C_7H_8)(\mathbf{1}) + 3/2\,H_2 \quad (1)$$

According to single-crystal structure analysis, $[Tb(cbz)_3(THF)_2](cbzH)(C_7H_8)$ (**1**) crystallizes in the monoclinic space group *P*2 (SI: Table S1, Figure S1, Supporting Information). **1** exhibits a central noncharged $Tb(cbz)_3(THF)_2$ molecule with additional, noncoordinating cbzH and toluene molecules in voids between the $Tb(cbz)_3(THF)_2$ molecules (**Figure 5**a). Herein, Tb^{3+} ions are trigonal-bipyramidally coordinated by three negatively charged $(cbz)^-$ and two THF ligands (Figure 5b). The $(cbz)^-$ ligands occupy the equatorial positions, whereas the sterically less demanding THF ligands are located in the axial positions. The Tb–N distances are 223(2) to 242(3) pm, which is slightly shorter than usually observed for *Ln*–N distances with the smaller lanthanides (233–254 pm).[21] The Tb–O distances are 232.2(10) and 235.3(9) pm. The longer Tb–O distances in comparison to the shorter Tb–N distances, despite the smaller size of THF than of cbz, can be attributed to the stronger attraction of the negatively charged $(cbz)^-$ ligands. The N–Tb–N angles of 117.8(6) to 124.3(11)° are in agreement with the trigonal-bipyramidal coordination. The O–Tb–O angles of 172.1(10) and 170.6(9) point to a certain tilting of the axially arranged THF ligands.

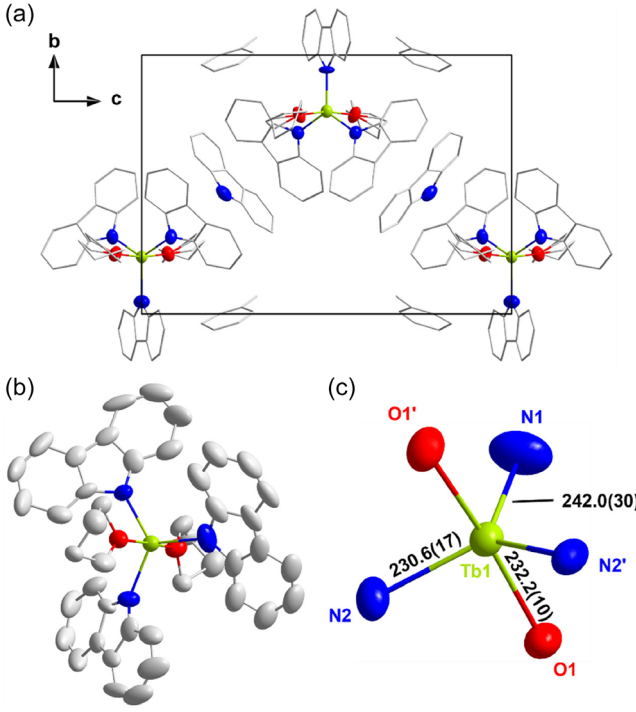

Figure 5. Crystal structure of $[Tb(cbz)_3(THF)_2](cbzH)(C_7H_8)$ (**1**): a) unit cell (see SI: figure S1, Supporting Information for anisotropic thermal ellipsoids of all atoms); b) molecular $Tb(cbz)_3(THF)_2$ unit; c) distorted trigonal bipyramidal TbN_3O_2 polyhedron with distances (in pm; H atoms and disorder not shown for clarity).

In the crystal structure, the $Tb(cbz)_3(THF)_2$ molecules, as the most voluminous building units, are arranged like in a primitive

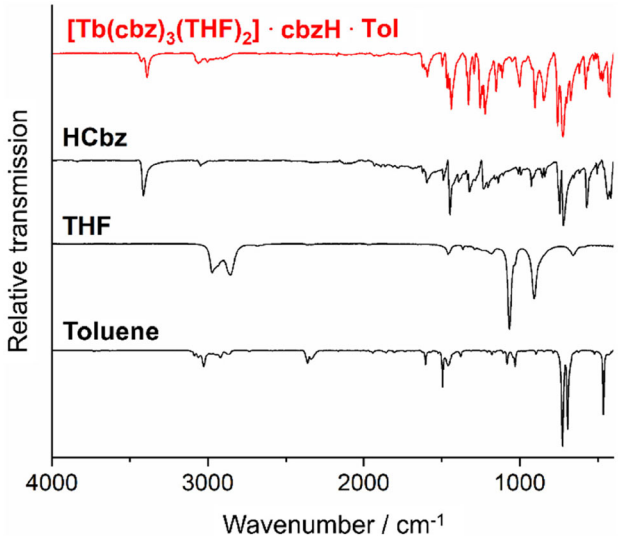

Figure 6. FTIR spectra of $[Tb(cbz)_3(THF)_2](cbzH)(C_7H_8)$ (**1**) with cbzH, THF, and toluene as references.

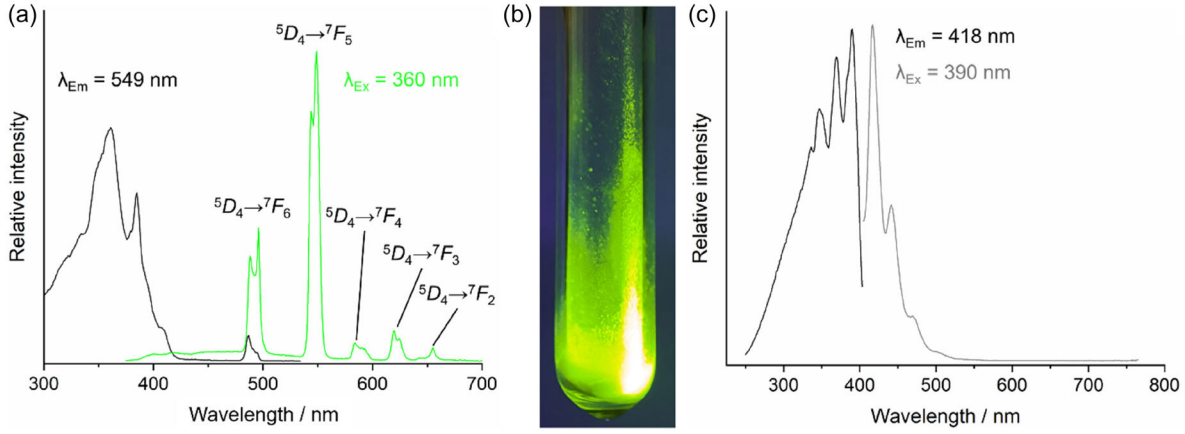

Figure 7. Luminescence of $[Tb(cbz)_3(THF)_2](cbzH)(C_7H_8)$ (**1**): a) excitation and emission spectrum (with respective term symbol for each emission line); b) photo of **1** with excitation at 366 nm; c) excitation and emission spectrum of free cbzH as a reference.

cubic packing. Noncoordinated cbzH and toluene molecules are located in the voids between the $Tb(cbz)_3(THF)_2$ molecules. In addition, it must be noticed that the THF molecules show positional disorder of the carbon atoms. This disorder was addressed with split-atom positions with 50% occupation for each atom.

The Tb–N distances and the absence of any other anion already point to the presence of negatively charged $(cbz)^-$ ligands in **1**. In addition, FTIR spectroscopy was involved. A comparison with spectra of free cbzH, THF, and toluene evidence their presence in **1** (**Figure 6**). Most characteristic are ν(C–O) of THF (1050, 910 cm^{-1}), ν(C=C) of cbzH (1440 cm^{-1}), δ(C=C) of cbzH and toluene (740-690 cm^{-1}), as well as the fingerprint region of cbzH (1500-1100 cm^{-1}). Specifically interesting is the N–H vibration at 3400 cm^{-1} (Figure 6). Although clearly visible for **1** and for the cbzH reference, the intensity of ν(N–H) is significantly lower for **1** as compared to free cbzH. This is in accordance with $(cbz)^-$ as a negatively charged ligand, as well as noncharged cbzH as a noncoordinating molecule in **1**.

Based on the observation that already the colorless single crystals show weak green emission in daylight, the luminescence properties of **1** were examined by photoluminescence spectroscopy (**Figure 7**). Accordingly, intense absorption of **1** occurred at 300–410 nm (Figure 7a). This absorption is very similar to pure cbzH (Figure 7c). Emission spectra of **1** show the characteristic $f \rightarrow f$-type emission lines of Tb^{3+} at 492, 549, 590, and 624 nm due to $^5D_4 \rightarrow {}^7F_{2,3,4,5,6}$ transitions (Figure 7a).[22] Here, it must be noticed that the emission of pure cbzH is significantly different and occurs at 400–500 nm (Figure 7c).[23] The fact that the emission spectrum of **1** does not show any emission of cbzH but only of Tb^{3+} indicates that the $(cbz)^-$ ligands serve as an efficient antenna. Finally, the absolute quantum yield of **1** was determined using the approach given by *Friend* et al.[24] This resulted in a value of 44.8 ± 0.03% at room temperature. Despite the intense emission of **1**, the quantum yield is much below many Tb^{3+}-based phosphors, showing quantum yields of up to 90%.[22] Although the excitation process can be considered to be efficient due to the allowed and intense antenna-type absorption of cbz, as well as due to the close distance between Tb^{3+} and the negatively charged $(cbz)^-$ ligands (Tb–N distance: 223(2) to 242(3) pm), most probably vibrational losses due to the THF ligands coordinated to Tb^{3+} cause a reduction of the quantum yield. Attempts to perform the reaction of Tb(0) nanoparticles with cbzH in the absence of THF, however, did not result in any crystalline product until now.

3. Conclusions

Highly reactive Terbium nanoparticles are realized in a liquid-phase synthesis by reduction of $TbCl_3$ with lithium naphthalenide in THF at room temperature. The as-prepared Tb(0) nanoparticles are monocrystalline and exhibit a particle diameter of 2.8 ± 0.4 nm with a narrow size distribution. Although being highly reactive (e.g., as powder samples when in contact with air), the Tb(0) nanoparticles are highly stable as suspensions in THF or toluene under inert conditions. Here, they are used as starting material for direct reaction with carbazole (cbzH) in toluene at 80 °C, resulting in the formation of Terbium carbazolate with a composition $[Tb(cbz)_3(THF)_2](cbzH)(C_7H_8)$ (**1**) with oxidation of Terbium and formation of H_2. **1** shows Tb^{3+} coordinated by three deprotonated $(cbz)^-$ ligands and two molecules of THF. **1** shows Tb^{3+}-driven emission of green light already in daylight. Photoluminescence spectroscopy indicates $(cbz)^-$ to serve as an antenna ligand for excitation, followed by Tb^{3+}-driven emission with a quantum yield of 44.8 ± 0.03% at room temperature. Besides the formation and characterization of **1** as a new compound, the redox approach with Tb(0) nanoparticles as a starting material can be an interesting option for chemical syntheses and the realization of new compounds, in general.

4. Experimental Section

General Aspects: All sample handling and reactions were performed under an argon atmosphere using standard Schlenk techniques and gloveboxes (MBraun Unilab, $O_2/H_2O < 1$ ppm). Prior to use, all glassware was evacuated ($p \leq 10^{-3}$ mbar), heated, and flushed with argon three times to remove all moisture.

Chemicals: Tetrahydrofuran (THF, Seulberger, 99%) and toluene (Seulberger, 99%) were refluxed over sodium with benzophenone

and distilled prior to use. Lithium metal (Alfa Aesar, 99%) was freshly cut under argon atmosphere prior to use. Carbazole (cbzH, Sigma–Aldrich, >95%), Terbium(III) chloride (Alfa Aesar, 99.9%), and naphthalene (Alfa Aesar, ≥ 99%) were used as purchased.

Tb(0) Nanoparticles: 6.9 mg of lithium (1.00 mmol, 3.03 eq), 135 mg of naphthalene (1.05 mmol, 3.18 eq), and 87.5 mg of Terbium(III) chloride (0.33 mmol, 1.00 eq) were added to 15 mL of THF. After intense stirring for 12 h at room temperature, the synthesis was finished and resulted in a deep black suspension. This suspension was centrifuged to separate the Tb(0) nanoparticles. To remove excess starting materials, naphthalene and LiCl, the nanoparticles were twice redispersed/centrifuged in/from 15 mL of THF. Finally, the Tb(0) nanoparticles were redispersed in THF or toluene or dried in vacuum (20 min) to obtain powder samples with a yield around 80%. Certain loss of nanoparticles can be ascribed to the purification process and predominantly nanoparticles sticking on the wall of the centrifuge tubes.

Specific attention must be paid to the handling of the Tb(0) nanoparticles as they show instantaneous combustion in air and even explosion when in contact with water or other oxidizing agents (see Video SV1, Supporting Information for the reactivity in air). Their reactivity was very comparable to the heavy alkali metals rubidium and cesium.

$[Tb(cbz)_3(THF)_2](cbzH)(C_7H_8)$ (1): 40.9 mg of the as-prepared Tb(0) nanoparticles (0.26 mmol, 1.00 eq) and 129 mg of carbazole (0.77 mmol, 3.00 eq) were added with 0.2 mL of toluene in a Schlenk tube. By heating for 3 days to 80 °C, the deep black color of the mixture lightened significantly. **1** was obtained as colorless crystals with a yield of about 70%. The crystals of **1** show certain emission of green light even under daylight.

Analytical Techniques: Further details related to the analytical equipment and single-crystal structure analysis are summarized in the Supporting Information. Further details of the crystal structure investigation may be obtained from the joint CCDC/FIZ Karlsruhe deposition service on quoting the depository number 2449804.

Acknowledgements

The authors thank Dr. Silke Wolf for finalizing the single-crystal structure analysis. A.R. and C.F. acknowledge financial support from the Deutsche Forschungsgemeinschaft (DFG, German Research Foundation) through the Collaborative Research Centre *"4f for Future"* (CRC 1573, project number 471424360), project A4.

Open Access funding enabled and organized by Projekt DEAL.

Conflict of Interest

The authors declare no conflict of interest.

Data Availability Statement

The data that support the findings of this study are available from the corresponding author upon reasonable request.

Keywords: carbazole · crystal structure · luminescence · terbium nanoparticles

[1] a) G. Kleinhans, A. J. Karhu, H. Boddaert, S. Tanweer, D. Wunderlin, D. I. Bezuidenhout, *Chem. Rev.* **2023**, *123*, 8781; b) D. Mueller, P. Saha, D. Panda, J. Dash, H. Schwalbe, *Chem. Eur. J.* **2021**, *27*, 12726.
[2] S. J. Malthus, S. A. Cameron, S. Brooker, *Coord. Chem. Rev.* **2016**, *316*, 125.
[3] L. S. Merz, J. Ballmann, L. H. Gade, *Eur. J. Inorg. Chem.* **2020**, 2023.
[4] a) T.-X. Liu, X. Wang, S. Xia, C. M. Chen, M. Li, P. Yang, N. Ma, Z. Hu, S. Yang, G. Zhang, et al, *Angew. Chem. Int. Ed.* **2023**, *62*, e202313074; b) J. C. Ott, H. Wadepohl, L. H. Gade, *Inorg. Chem.* **2021**, *60*, 3927; c) A. Hinz, *Angew. Chem. Int. Ed.* **2020**, *59*, 19065.
[5] a) C.-H. Yu, C. Zhu, X. Ji, W. Hu, H. Xie, N. Bhuvanesh, L. Fang, O. V. Ozerov, *Inorg. Chem. Front.* **2020**, *7*, 4357; b) I. Buslov, J. Becouse, S. Mazza, M. Montandon-Clerc, X. Hu, *Angew. Chem. Int. Ed.* **2015**, *54*, 14523.
[6] a) C. Poriel, J. Rault-Berthelot, *Adv. Funct. Mater.* **2020**, *30*, 1910040; b) Q. Zhang, N. Li, X. Wan, X.-F. Song, Y. Zhang, H. Liu, J. Miao, Y. Zou, C. Yang, K. Li, *Angew. Chem. Int. Ed.* **2025**, *64*, e202419290; c) M. Gernert, L. Balles-Wolf, F. Kerner, U. Mueller, A. Schmiedel, M. Holzapfel, C. M. Marian, J. Pflaum, C. Lambert, A. Steffen, *J. Am. Chem. Soc.* **2020**, *142*, 8897; d) M.-Y. Leung, M.-C. Tang, W.-L. Cheung, S.-L. Lai, M. Ng, M.-Y. Chan, V. Wing-Wah Yam, *J. Am. Chem. Soc.* **2020**, *142*, 2448.
[7] a) S. Cai, H. Shi, Z. Zhang, X. Wang, H. Ma, N. Gan, Q. Wu, Z. Cheng, K. Ling, M. Gu, et al, *Angew. Chem. Int. Ed.* **2018**, *57*, 4005; b) T. Ma, K. Li, J. Hu, Y. Xin, J. Cao, J. He, Z. Xu, *Inorg. Chem.* **2022**, *61*, 14352.
[8] a) L. Shi, M. Qi, L. Han, W. Liang, A. M. Kirillov, W. Dou, W. Liu, L. Yang, *Inorg. Chem.* **2025**, *64*, 5086; b) L. Gajecki, D. J. Berg, J. Hoenisch, A. G. Oliver, *Dalton Trans.* **2018**, *47*, 15487; c) D.-H. Chen, L. Lin, T.-L. Sheng, Y.-H. Wen, X.-Q. Zhu, L.-T. Zhang, S.-M. Hu, R.-B. Fu, X.-T. Wu, *New J. Chem.* **2018**, *42*, 2830; d) W. Xie, S.-R. Zhang, D.-Y. Du, J.-S. Qin, S.-J. Bao, J. Li, Z.-M. Su, W.-W. He, Q. Fu, Y.-Q. Lan, *Inorg. Chem.* **2015**, *54*, 3290.
[9] R. Zhong, X. Yu, R. Zou, *Inorg. Chem. Commun.* **2015**, *61*, 173.
[10] K. Mueller-Buschbaum, C. C. Quitmann, *Z. Anorg. Allg. Chem.* **2003**, *629*, 1610.
[11] a) W. J. Evans, G. W. Rabe, J. W. Ziller, *Organometallics* **1994**, *13*, 1641; b) G. Deacon, C. Forsyth, R. Newham, *Polyhedron* **1987**, *6*, 1143.
[12] K. Müller-Buschbaum, C. C. Quitmann, *Eur. J. Inorg. Chem.* **2004**, 4330.
[13] a) Y. Hu, R. S. H. Khoo, J. Lu, X. Zhang, J. Zhang, *ACS Appl. Mater. Interfaces* **2022**, *14*, 41178; b) R. Mu, Y. Ran, J. Du, X. Wu, W. Nie, J. Zhang, Y. Zhao, H. Liu, *Polyhedron* **2017**, *124*, 125; c) T. Yu, R. Liang, Y. Zhao, Y. Song, B. Gao, M. Li, L. Min, H. Zhang, D. Fan, *Polyhedron* **2015**, *85*, 789; d) S. Raphael, M. L. P. Reddy, K. V. Vasudevan, A. H. Cowley, *Dalton Trans.* **2012**, *41*, 14671.
[14] F. Gyger, P. Bockstaller, D. Gerthsen, C. Feldmann, *Angew. Chem. Int. Ed.* **2013**, *52*, 12443.
[15] C. Schöttle, P. Bockstaller, D. Gerthsen, C. Feldmann, *Chem. Commun.* **2014**, *50*, 4547.
[16] A. Egeberg, T. Block, O. Janka, O. Wenzel, D. Gerthsen, R. Pöttgen, C. Feldmann, *Small* **2019**, *15*, 1902321.
[17] a) D. Bartenbach, O. Wenzel, R. Popescu, L.-P. Faden, A. Reiß, M. Kaiser, A. Zimina, J.-D. Grunwaldt, D. Gerthsen, C. Feldmann, *Angew. Chem. Int. Ed.* **2021**, *60*, 17373; b) C. Schöttle, P. Bockstaller, R. Popescu, D. Gerthsen, C. Feldmann, *Angew. Chem. Int. Ed.* **2015**, *54*, 9866.
[18] A. Reiß, A. Appenzeller, J. Baur, J. Wenzel, R. Popescu, K. Beuthert, S. Dehnen, Y. M. Eggeler, F. Breher, W. Klopper, C. Feldmann, *Small* **2025**, *21*, 2503498.
[19] A. E. Curzon, H. G. Chlebek, *J. Phys. F.* **1973**, *3*, 1.

[20] a) L.-P. Faden, A. Reiß, R. Popescu, C. Donsbach, J. Göttlicher, T. Vitova, D. Gerthsen, C. Feldmann, *Inorg. Chem.* **2024**, *63*, 1020; b) C. Ritschel, C. Donsbach, C. Feldmann, *Chem. Eur. J.* **2024**, *30*, e202400418.
[21] K. Müller-Buschbaum, C. C. Quitmann, *Inorg. Chem.* **2003**, *42*, 2742.
[22] G. Blasse, B. C. Grabmeier, *Luminescent Materials*, Springer, Berlin **1994**.
[23] R. P. Kreher, *Hetarene 1*,Thieme, Stuttgart **1994**.
[24] J. C. De Mello, H. F. Wittmann, R. H. Friend, *Adv. Mater.* **1997**, *9*, 230.

Manuscript received: May 19, 2025
Revised manuscript received: July 24, 2025
Version of record online:

